The Journal of the Korean Society of Oceanography
Vol. 30, No. 6, pp. 550-564, December 1995

Temporal and Spatial Characteristics of Surface Winds over the Adjacent Seas of the Korean Peninsula

SANG-KYU HAN*, HEUNG-JAE LIE** AND JUNG-YUL NA*
*Department of Earth and Marine Sciences, Hanyang University, Ansan, 425-791, Korea
**Physical Oceanography Division, Korea Ocean Research and Development Institute, Ansan, 425-600, Korea

한국 주변해역에서의 해상풍의 시공간적 특성

한상규* · 이흥재** · 나정열*
*한양대학교 지구해양과학과
**한국해양연구소 해양물리연구부

The temporal and spatial characteristics of wind fields over the neighbouring seas of the Korean peninsula are investigated using 10-years daily wind data during 1978~1987 which have been spatially smoothed and low-pass filtered. Long term annual and monthly means are examined for synoptic patterns and spectral analyses are made for temporal variability and spatial coherence. Spatial patterns of the annual mean wind stress and curl have a strong resemblance with those of monthly means during the winter season. Two outstanding periodicities are observed at 1 and 2 cycles per year. The synoptic winds over the study area are highly coherent at both the annual and semi-annual periodicities. However, each basin has its own characteristic spatial pattern. For instance, the prevailing wind during the winter season is northerly over the northern East Sea (ES), Yellow Sea (YS), and northern East China Sea (ECS), while it is northwesterly over the southern ES and northesterly over the northern ES and southern ECS. At the same time, the wind stress curl is positive over the northern ES and southern ECS, while it is negative over the southern ES, YS and northern ECS. On the other hand, the wind field during the summer season, with its strength being much reduced, is completely different from that during the winter season, and frequent passage of tropical storms provokes large temporal variability over ECS. One remarkable point is that the annual cycle, dominated by the Siberian High, tends to propagate from northeast to southwest, i.e., from northern ES toward southern ES, YS and ECS, while the semi-annual cycle propagates in the opposite direction, from southwest to northeast. The semi-annual periodicity may reflect development of extratropical cyclones in spring and fall which frequently cross the Korean peninsula. In higher frequencies, there are no dominant periodicities, but local winds over YS and ES are highly correlated for frequencies larger than 0.1 cycles per day and phase difference increases linearly with frequency. This linear increase of phase corresponds to phase speed of 550 and 730 km/d at 0.1 and 0.3 cpd, respectively. The phase speed is apparently coincident with moving speed of extratropical cyclones across the Korean peninsula in the west-east direction.

공간적으로 평활화하고 저주파 필터를 적용한 1978년부터 1987년까지 10년간의 일별 해상풍 자료를 이용하여 한국 주변해역에서의 해상풍의 시 · 공간적 분포특성을 연구하였다. 종관적 분포형태를 위해 해상풍의 연평균과 월평균 분포특성을 검토하였고, 시간적 변동성과 공간적 상관성을 위해 스펙트럼 분석을 하였다. 연평균 wind stress와 curl의 공간형태는 겨울철 월평균 형태와 매우 닮았다. 일년 및 반년주기성이 뚜렷하다. 연구해역에서 종관적 바람은 일년 및 반년 주기에서 공간적 상관성이 매우 높으나 각 해역별로 특징적 공간분포를 보인다. 예를 들면, 겨울철 바람은 동해북부, 황해와 동중국해 북부에서는 북풍이 우세한 반면, 동해남부에서는 북서풍이, 동중국해 남부에서는 북동풍이 우세하다. 또한 curl의 경우는 동해북부와 동중국해 남부에서는 양의 값을 보이나 동

해남부와 황해 그리고 동중국해 북부에서는 음의 값을 보인다. 한편, 세력이 대단히 약해지는 여름철 바람은 겨울철 바람과 아주 다르고 열해성 저기압의 빈번한 통과로 동중국해 해상에서 시간변동이 커진다. 시베리아 고기압이 큰 영향을 끼치는 연변동은 북동에서 남서로, 즉 동해북부에서 동해남부 및 황해와 동중국해로 전파되는 경향을 보이나, 반년변동은 반대방향인 남서에서 북동으로 전파되는 점은 주목할 만하다. 반년 주기성은 한반도를 서에서 동으로 횡단하는 온대성 저기압이 봄과 가을에 발달하는 것을 나타내는 것으로 판단된다. 단주기 영역에서는 뚜렷한 주기성이 나타나지 않지만, 0.1 cycles per day (cpd) 이상에서는 황해와 동해의 지역풍이 공간적 상관성이 높고 위상도 주파수에 선형적으로 증가한다. 이러한 선형적 증가는 0.1, 0.3 cpd에서 550, 730 km/d의 위상속도에 해당하며 위상속도는 한반도를 서-동으로 통과하는 온대성 저기압의 이동속도와 외형적으로 일치한다.

INTRODUCTION

Surface winds over the ocean play a very important role not only to generate wind-driven current, but also in heat exchanges between ocean and atmosphere. However, the surface wind used for the ocean circulation and the heat exchange are usually estimated by indirect methods because of lack of observed wind data and scarce spatial coverage. Dynamical calculations from the synoptic surface pressure fields (Willebrand, 1978), numerical prediction (Chave *et al.*, 1991), and statistical computation from pilot-chart (Hidaka, 1958 ; Hellerman, 1967) or ships-of-opportunity data (Wyrtki and Meyers, 1975, 1976 : Bunker, 1976 ; Kutsuwada, 1982) are enumerated as the representative indirect methods.

Wind data observed at coastal weather stations along the Korean coast and at two fixed buoy stations of the Japan Meteorological Agency have been frequently used to study characteristics of the wind field or for intercomparison between observed and estimated winds. In general, the wind data at the coastal stations are seriously contaminated due to the topographic effect of land and contain significant diurnal signals of land-sea breeze, so the data are not very useful for estimating the wind field on the sea surface in the Korean neighbouring seas. The surface wind field over the Korean neighbouring seas have been studied mostly on the basis of indirectly estimated data. Kim and Choi (1986) computed monthly geostrophic winds over the East Sea from 55 years monthly mean atmospheric pressure data during 1881~1935 and they described general features of long-term monthly wind stresses and curls. Na *et al.* (1992, briefly NSH hereafter) complied comprehensive database by applying Cardone model (1969) to 12 hourly weather charts and ten-day mean sea surface temperature (SST) during 1978~1987 and presented spatial patterns of long-term monthly wind stress as well as wind stress curl in the East Sea (ES), Yellow Sea (YS), and the northern East China Sea (ECS). Kang *et al.* (1994) computed surface winds around the Korean peninsula for a three year period of 1985~1987 using daily pressure data of the European Center for Medium Range Forecast and monthly SST data of the National Meteorological Center in USA.

The previous studies on the surface wind in the Korean neighbouring seas commonly pointed out the outstanding seasonality of the prevailing wind field : northerly wind in winter and southerly wind in summer. However, spatial structures and magnitude of the local wind fields of the previous studies are not identical, especially for the curl fields. For instance, the wind stress curl in Wonsan Bay in winter is positive (cyclonic wind) in NSH (1992), but negative (anticyclonic) in the other studies (Kim and Choi, 1981; Kang *et al.*, 1994). On the other hand, the curl in YS in winter is negative over the whole basin in Kang *et al.* while according to NSH the positive curl appears locally in the eastern YS along the Korean coast. Fig. 5. Monthly variation of zonally averaged wind stress and curl. (a) the East Sea and (rean coast. The significant differences between the studies may result mainly from the spatial resolution of input data.

The previous studies have paid much attention to the general pattern of long-term annual and monthly means of wind stresses and curls. Therefore, we attempt to investigate basic temporal and spatial characteristics of the wind fields and to compare wind fields of the three different basins, ES, YS,

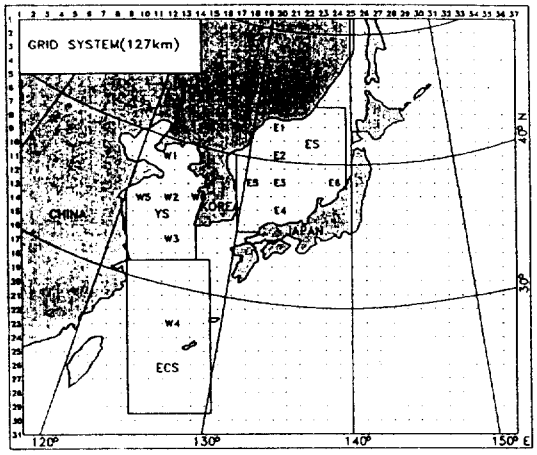

Fig. 1. Study area and grid system for computation of sea surface wind. Grids E1-E6 and W1-W6 are selected as representative ones for spectral and cross-spectral analysis.

and ECS for spatial correlation. The database used for this study is an extended one of NSH, complemented to completely cover the Korean neighbouring seas and part of the northwestern Pacific. The original database of NSH does not cover the whole ECS.

DATABASE AND PROCESSING

We extended the wind database compiled by NSH to cover the whole neighbouring seas of Korea and part of the northwest Pacific. The spatial coverage is 20° to 50° N and 120° to 150° E (Fig. 1). The computation of surface wind was performed by Cardone model, described in detail in NSH. The new database composes of gridded time series for a period of 10 years between 1978 and 1987. The grid spacing is 127 km and the sampling interval is 12 hours, so the data intervals are narrow and short enough to resolute local wind structures and temporal variations with high statistical reliability.

The 12 hourly wind data are first spatially smoothed to reduce erroneous values, possibly due to small scale fluctuations comparable to the grid size. Smoothed time series at a given point are calculated using observed values at the grid point under consideration and eight neighbouring grids according to the following formula,

$$F(0,0) = \frac{1}{36}\{16f(0,0) + 4f[(1,0) + f(-1,0) + f(0,1) + f(0,-1)] + [f(1,1) + f(-1,1) + f(1,-1) + f(-1,-1)]$$

where F (0,0) is the smoothed value of wind components at the given grid point (0,0) and f (i,j) is value at grid (i,j). The smoothed time series are then low-passed to remove high frequency signals above 0.5 cpd, possibly caused by the land-sea breeze. The land-sea breeze with a periodicity of 1 cpd and amplitude of several m/s is known to be spatially variable around the Korean peninsula and its strength exceeds sometimes that of the synoptic wind (Kim and Jhun, 1992; Park and Park, 1992). The effect of breeze is effectively filtered out by the low-passed filter.

The low-passed daily time series are subject to the basic statistical and spectral analysis. Spectrum and cross-spectrum analysis are made at pre-selected grid points shown in Fig. 1. The piece-average method of Gonella (1972) is used for the spectra. For the piece-average analysis, the ten years long time series are divided into 8 overlapped piece, each piece being a three years long time series. Spectrum and cross-spectrum of each piece are first estimated and then averaged to get the mean spectrum. The 90 % confidence interval for spectrum and the 90 % confidence limit for coherence are estimated and marked in the corresponding spectra.

ANNUAL AND MONTHLY MEAN WIND FIELDS

Long-term Annual Means

Fig. 2 shows the ten year long-term mean of surface wind stress with its standard deviation. The mean wind stress is relatively strong with magnitude of the order of 0.4 dyne/cm^2 (hereafter the unit of dyne/cm^2 is omitted) over the Korean neighbouring seas, but it is very weak in the southeastern study area, south of 30° N and east of 130° E. The spatial patterns of mean wind fields over the three

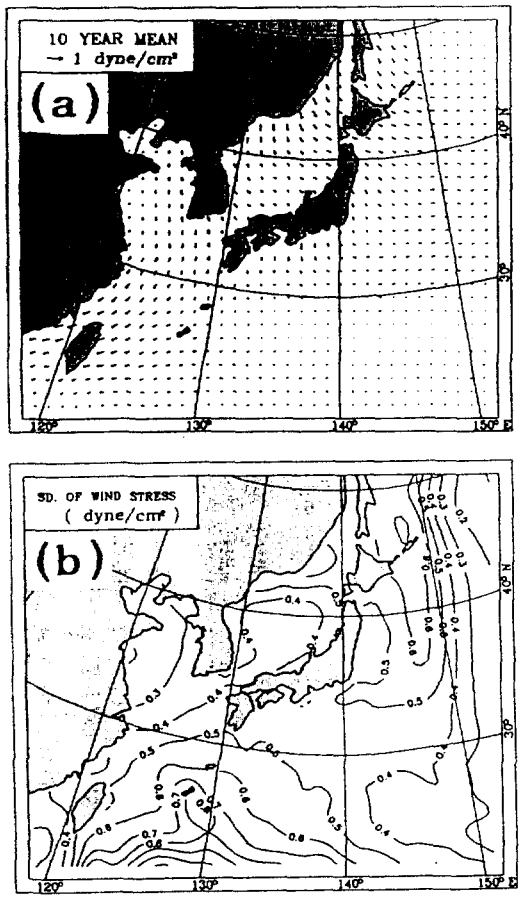

Fig. 2. Long-term mean and standard deviation of surface wind stress over the Korean neighbouring seas. (a) Mean wind stress and (b) standard deviation. The unit is dyne/cm^2.

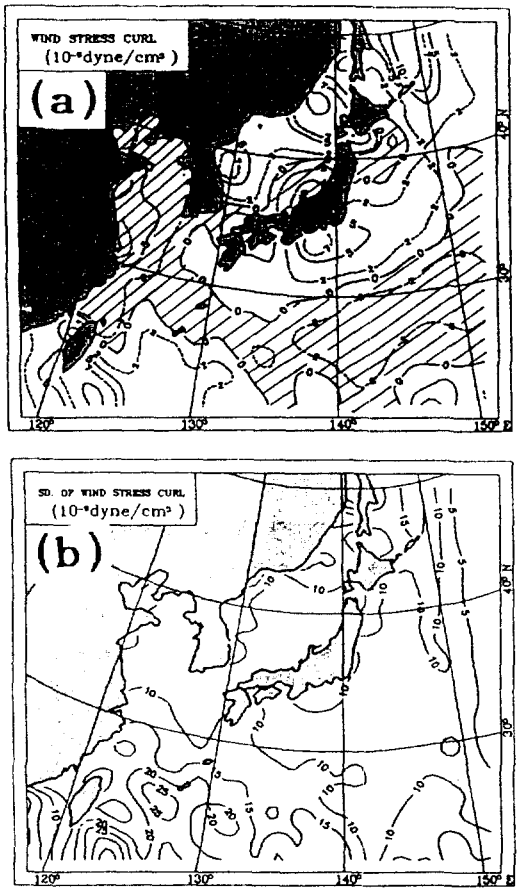

Fig. 3. Long-term mean and standard deviation of surface wind stress curl over the Korean neighbouring seas. (a) Mean wind stress curl and (b) standard deviation. The unit is 10^{-9} dyne/cm^3 and shaded area indicated negative curl.

basins ES, YS, and ECS are different from one basin to another in terms of prevailing direction and strength. The standard deviation exceeds the mean value, reflecting important variability in time. Prevailing winds over ES is northerly with strong stress of about 0.5 in the northern basin north of 40° N and northwesterly in the southern basin with weaker stress less than 0.4. Northerly winds are predominant over the whole YS and the northern ECS north of 30° N, while over the southern ECS, the northeasterly wind is prevailing with stress comparable to that over the northern ES. Over the southwestern study area, the easterly wind is prevailing, but its strength is very weak. Over the YS and the northern ECS, the west-east gradient of wind stresses is remarkably large, even through the northerly wind dominates the whole area. The wind seems to be divergent around 130° E in ECS, with northeasterly to the west of 130° E and weaker northwesterly to the east.

The standard deviation is a good indicator showing magnitude of temporal variation. It decreases with increasing latitudes, with an exception in the northeastern ES. Standard deviation of long-term monthly means (Fig. 4 of Lie *et al.*, 1994) increases with increasing latitude during the winter season, but it decreases with latitude during the summer sea-

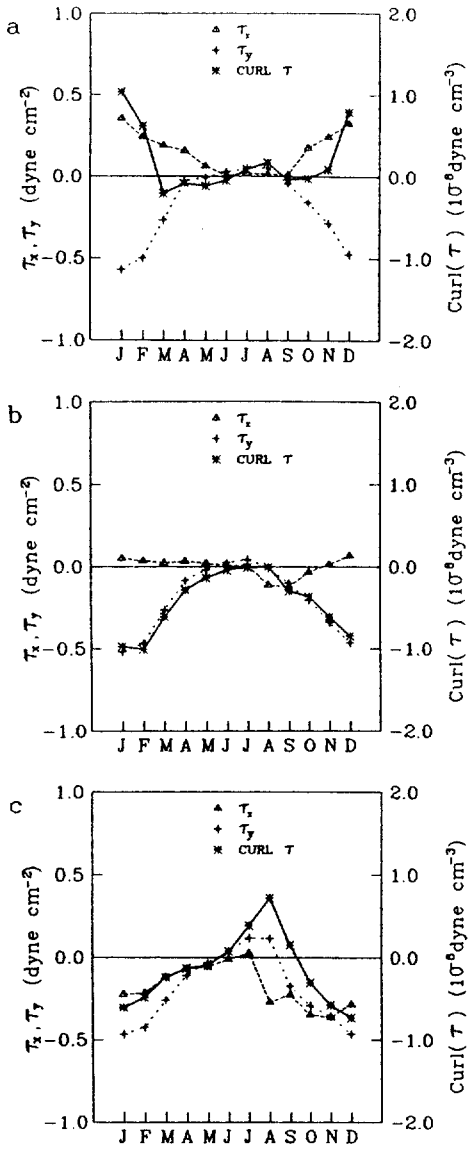

Fig. 4. Monthly variation of eastward (▲) and northward (⊕) wind stress, and wind stress curl (*), spatially averaged over each basin. (a) the East Sea, (b) the Yellow Sea, and (c) the East China Sea.

son, mainly due to frequent passage of typhoons. It is also noteworthy to see that the long-term annual mean has a pattern very similar to the long-term monthly mean during the winter season (Fig. 2 in NSH and Fig. 3 in Lie *et al.*, 1994). This may be explained through our understanding of weather patterns over the study area in different seasons. In winter, the eastern Asia is dominated by the Siberian High which does not move away, instead excursing southeastward as it develops. On the other hand, the weather patterns in spring and fall moves relatively faster and the Siberian High weakens sharply. In summer, the tropical maritime High develops and advances to the north, but its strength is much weaker than that of the Siberian High. As a result, the annual mean wind field has a weather pattern similar to that in winter, northerlies around the Korean peninsula. Standard deviations of the unfiltered time series are several times larger than those of the smoothed, filtered data in Fig. 2, especially in the coastal region, so low-pass filtering is an inevitable step of removing temporal variability.

Fig. 3 is the long-term annual mean of wind stress curl and its standard deviation. The general pattern of mean curl field resembles that of NSH (Fig. 4), but the magnitude is smaller than that of NSH, mainly due to effects of spatial smoothing and low-pass filtering. The mean curl is less than 8×10^{-9} dyne/cm^3 (hereafter 10^{-9} dyne/cm^3 is omitted) everywhere in the study area, with an exception in an area east Hokkaido where it exceeds 10. The curl over ES is positive over the northern and central region, but negative in the Honshu coastal area. Two positive curl maxima are observed in Wonsan Bay and the northeastern ES, with magnitude smaller by 30% than that of NSH. This agrees fairly well with the meteorological observations that cyclonic vortex or wind shear are frequently observed near Wonsan Bay area (personal communication from T.-Y. Lee) and that cyclogeneses are also frequently observed over the ocean east of Hokkaido. The negative curl dominates the whole YS with a minimum value in the Chinese coast between the Shantung peninsula and Changjing River mouth. The positive curl in the eastern YS, reported in NSH, is a result that they did not apply spatial smoothing to the serial data. The wind over ECS is dominated by negative curl, but the positive curl is observed in deep ocean region east of Taiwan and south of Japanese Islands. The standard deviation of the curl tends to increase toward the

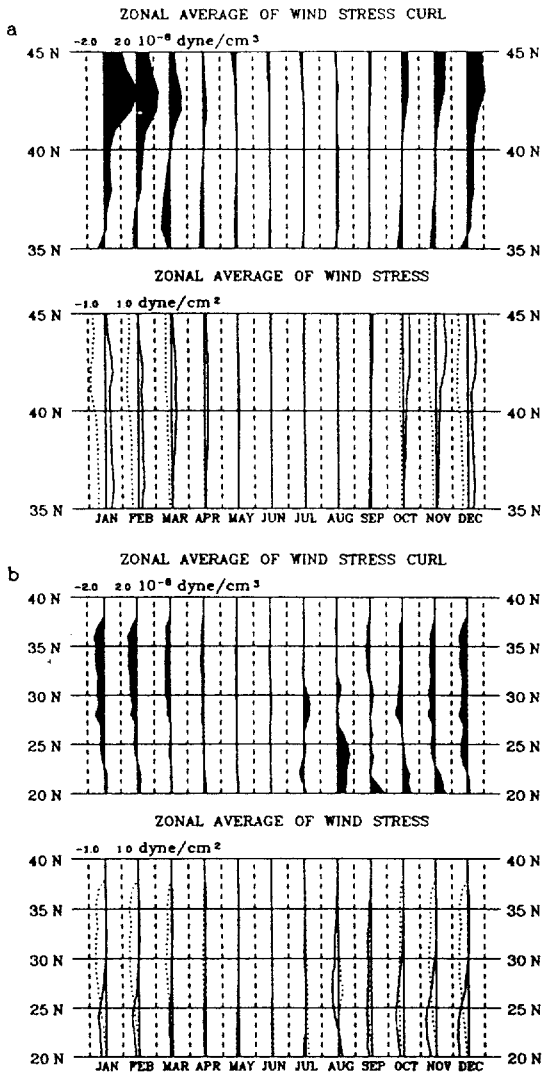

Fig. 5. Monthly variation of zonally averaged wind stress and curl. (a) the East Sea and (b) the Yellow and East China Seas. Solid and dashed lines for the wind stress correspond to the northward and eastward wind components, respectively.

south as that of the long-term mean stress.

To see characteristic wind fields for ES, YS, and ECS, long-term monthly means of wind stress and curl over each basin are spatially averaged (Fig. 4). During the cold season, the prevailing wind is northwesterly with positive curl over ES, northerly with negative curl over YS, and northeasterly with negative curl over ECS, respectively. During the warm season, the wind is very weak over both ES and YS, while southwesterly wind with positive curl is prevailing over ECS, through its magnitude is not so strong as the northeasterly during the cold season. Thus, the characteristic wind fields in the neighbouring seas are different from one basin to another one.

Long-term Monthly Means

Monthly variations of the synoptic wind are examined using long-term monthly means of zonal wind stress and curl (Fig. 5). In Fig. 5 the upper two figures present the zonal wind stress and curl over ES and the lower two over YS and ECS. Solid and dashed lines corresponding respectively to the eastward and northward winds. Over ES, the northwesterly wind is prevailing from October to April of the following year, with positive curl in the northern area and negative in the southern area. The demarcation zone where the curl sign changes advances toward the south from September through January during the developing phase of the northerly wind, but retreats to the north from January to April during the weakening phase. The wind in January is strongest with maximum positive curl, while during the summer the wind stress and curl are much weakened. Over YS and ECS, the prevailing winds in winter are northerly over the northern basin north of 30° N and northeasterly in the southern ECS, and the curl sign is negative. In the deep ocean region south of the Kuroshio and east of Taiwan, the curl changes to the positive sign, even through the northerly wind is still dominant. As seen for ES, the demarcation zone is displaced northward or southward between 22° and 28° N, moving to the south (north) when the northerly wind is strengthened (weakened). During the summer season, the prevailing winds are southerly or southeasterly, with mean speed being much reduced. The monthly means of curl are small with magnitude less than 3 over YS and ES, while over ECS they are positively large with important variation in time and space. The positive curl and large temporal variability are related to the subtropical wind system, especially to

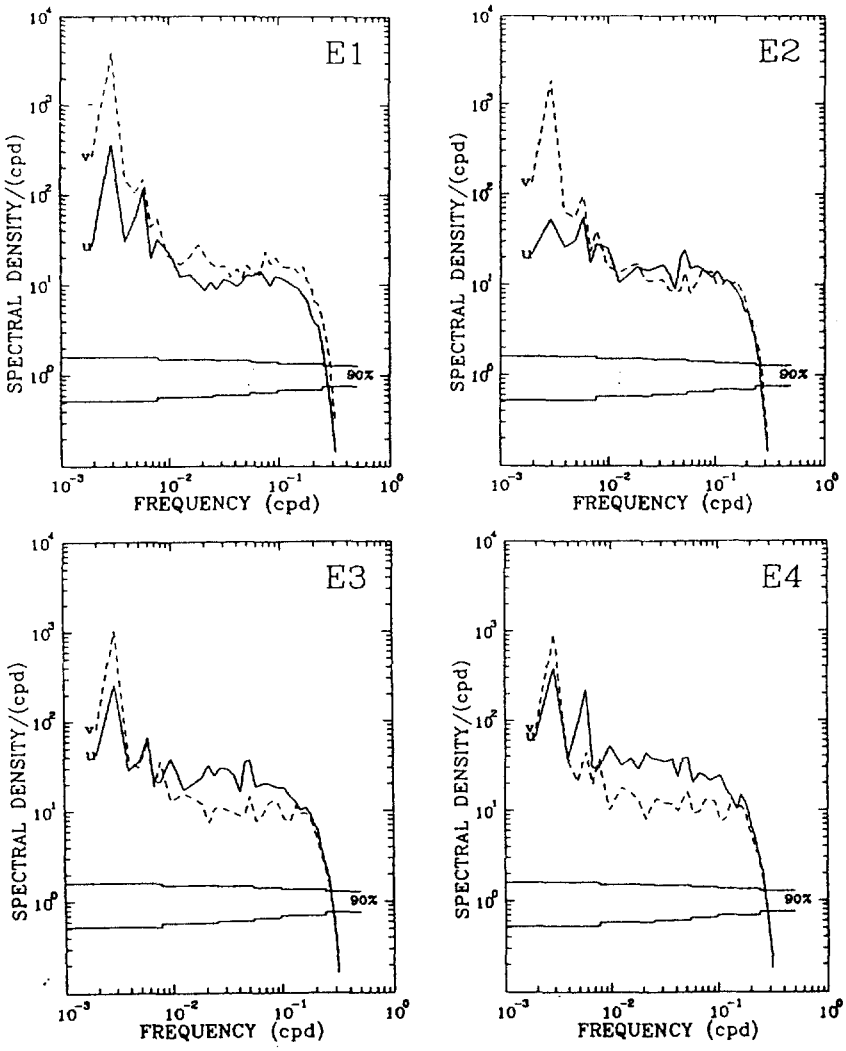

Fig. 6. Spectra of wind stresses at grids E1-E6 in the East Sea. Solid and dashed lines correspond to the eastward and northward wind components, respectively. The grids are marked in Fig. 1.

frequent passage of typhoons over ECS during the summer season.

TEMPORAL AND SPATIAL CHARACTERISTICS

In the previous section, the wind fields over the Korean neighbouring seas seen to be spatially different from one basin to another one, with an outstanding annual cycle. Therefore, the temporal and spatial characteristics are quantitatively examined by the piece-average spectral and cross-spectral analysis of demeaned, low-passed series of wind speed at the pre-selected grids marked in Fig. 1.

Wind Spectra

Fig. 6 is spectra of the two wind stress components at six representative grids of ES. The grids are located on lines crossing ES in the north-south (north wind hereafter) and west-east directions (east

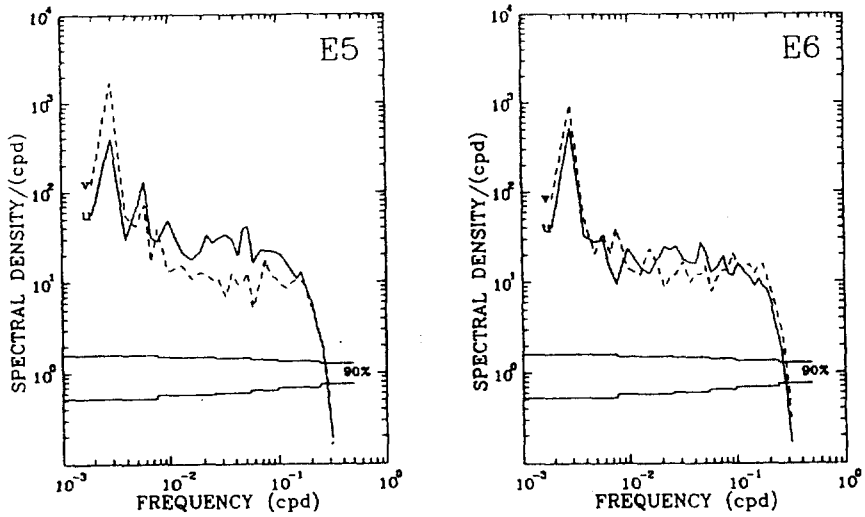

Fig. 6. Contined.

wind hereafter). Spectral density is larger than 10 $(cm/s)^2/cpd$ in the frequency range lower than 0.1 cpd. Significant spectral peaks are observed at two low frequency bands of 1 and 2 cycles per year (cpy) in which a large portion of the total spectral energy is concentrated. The energy concentrated in the higher frequency range 0.01~0.1 cpd is lower, but its level is nearly constant. The energy level for the north wind an 1 cpy is one order higher than that at 2 cpy and decreases southward and eastward, so the density at 1 cpy is maximum at grid E1 near the Siberian coast and minimum at grids E4 and E6 off the northern coast Honshu. For the east wind, the density at 1 cpy increases from north to south, in the opposite direction of the north wind and it is always lower than that of north wind through the levels for both winds are comparable at a southeastern grid E6. The density of east wind at 2 cpy exceeds that of the north wind at the same frequency only for E5 and E6 located in the southwestern basin. This may indicate that the semi-annual periodicity of the east wind is characteristic of the wind field in the southwestern ES.

Wind spectra for YS and ECS are presented in Fig. 7. The spectra for the north wind have a pattern similar to those for ES, showing the energy peak at 1 cpy. The spectral peak is one-order higher than that for the east wind at all grids, except that at W4 in ECS. The energy level at 1 cpy on the Korean side is higher than that on the Chinese side. The east wind has two peaks at 1 and 2 cpy and the energy level at 2 cpy for the east wind is higher than that at 1 cpy for grids W2, W3, and W5, located in the central and western YS. The spectra show that the synoptic wind is spatially variable even over YS about 500 km wide. At W4 in ECS, the annual variation is outstanding, with the same magnitude for both winds.

The spectra for north wind show that the annual cycle is the most important signal at all grids considered. However, the east wind has two peaks at 1 and 2 cpy at all grids through the density level is dependent upon location of grids. The annual variation is found to be more important at grids where the mean wind is stronger. The semi-annual periodicity is significantly high, especially in the southwestern ES and YS, but its spectral energy is not so large as that of the annual cycle. The annual cycle is closely related with the synoptic wind system controlled by the Siberian High, while the semi-annual cycle may represent transit phases during spring and autumn when the study area is influenced by more mobile pressure systems. Extratropical cyclones are known to develop in spring and fall, crossing frequently the Korean peninsula (Jung and Jhun, 1977). However, the semi-annual

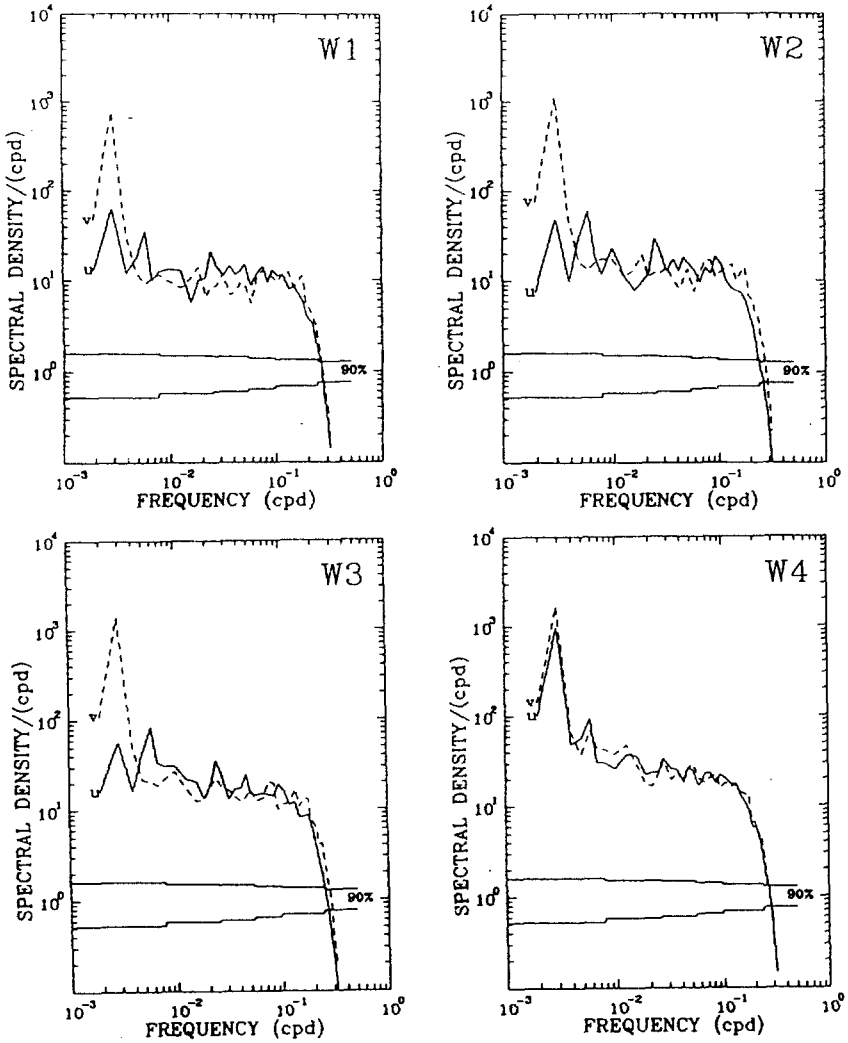

Fig. 7. Spectra of wind stresses at grids W1-W6 in the Yellow and East China Seas. Solid and dashed lines correspond to the eastward and northward wind components, respectively. The grids are marked in Fig. 1.

cycle, characterized by a clockwise rotation motion (Lie *et al.*, 1995), should be clearly elucidated in connection with the development of cyclones during the transit periods.

Cross-spectra

The spatial characteristics of wind field are investigated by computing the coherence and phase difference between pairs of grids shown in Fig. 1. As the case for the spectral analysis, the piece-average method was used to estimate the cross-spectrum.

Fig. 8 displays coherences and phase differences for the wind speeds between grids located in ES. The solid and dashed lines correspond respectively to east and north winds and the thick solid line marks 90 % confidence limit. Between winds at the central and northern ES (grids E3 and E1), the coherence for the north wind is significantly high with small phase difference over the full range of frequency, with an exception of frequency bands of 0.02~0.06 cpd, but the coherence for east wind is significant only at of 1 and 2 cpy, with relatively

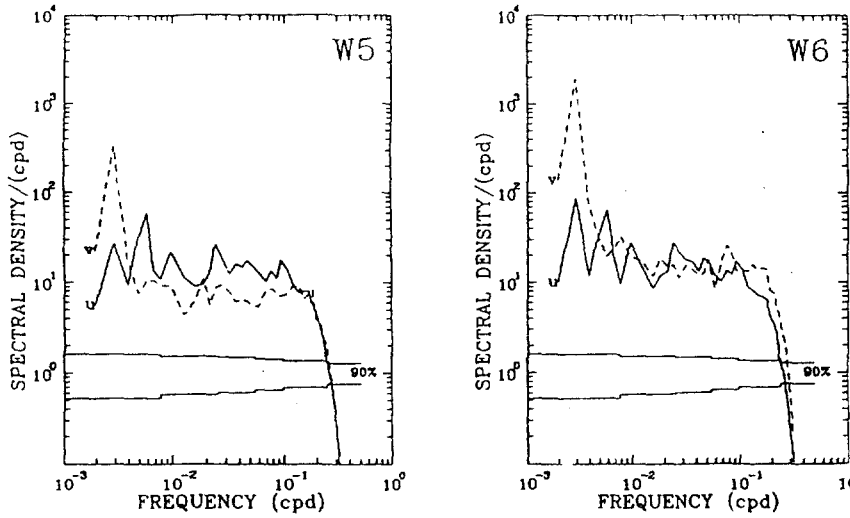

Fig. 7. Continued.

large phase differences. The positive phase of about 160 degrees at 1 cpy for the east wind means that the east wind at E1 advances that at E3 at 1 cpy, but the negative phase of about 140 degrees at 2 cpy means that the east wind at E3 leads that at E1. Therefore, the near out-of phase of the east wind between E1 and E3 reflects that the east wind direction is almost opposite. The opposite direction may be related to the variation of the east wind across the convergence over the East Sea (called open as the Japan Sea convergence zone) in the winter time. Northerlies and westerlies are found in the northern and southern parts of ES, respectively. Between the central and southern ES (E3 and E4), the coherences for both winds are much higher than the confidence limit over the full frequency range, with slight phase differences. This indicates that the central and southern ES is under influence of the same wind system. For the western and eastern ES (E5 and E6), the north winds are significantly correlated in frequencies lower than 0.01 cpd and higher than 0.1 cpd, but the east winds are highly correlated over the long distance in the east-west direction in the full range. The east winds between E1 and E4 are poorly correlated, except at the two peak frequencies of 1 and 2 cpy (Lie *et al.*, 1994).

The coherences and phase differences for YS are presented in Fig. 9. The north wind is well correlated along the north-south line (grids W1, W2, and W3), but the east wind between the western and eastern YS (W5 and W6) is significant only in the low frequencies less than 2 cpy. The east wind is correlated along the north-south line, but the coherence is lower than that for the north wind. It is noteworthy to see that the east winds at W5 and W6 are closely correlated with higher coherence than that for the north wind as seen in the case for ES. The three cross-spectra of the north wind show very high coherence and negligibly small phase at 1 cpy, which implies that the annual variation over the whole YS is controlled mainly by the same wind system.

YS and ES are geographically separated by the north-south stretch of the Korean peninsula. Spatial correlation between YS and ES can be roughly estimated in terms of coherence and phase difference at two pairs of grids, W1-E1 near the northern coastal area and W2-E3 in the central area (Fig. 10). For both pairs, the north wind at 1 cpy is spatially very coherent with no phase difference, but the east wind is significantly correlated only at the two peak frequency with certain phase difference. The east wind at E1 advances that at W1 for 1 cpy, but lags behind W1 for 2 cpy. For the pair of W2-E3, the situation is reversed; the east wind and E3 lags behind that at W2 for 1 cpy and advances W2 at 2

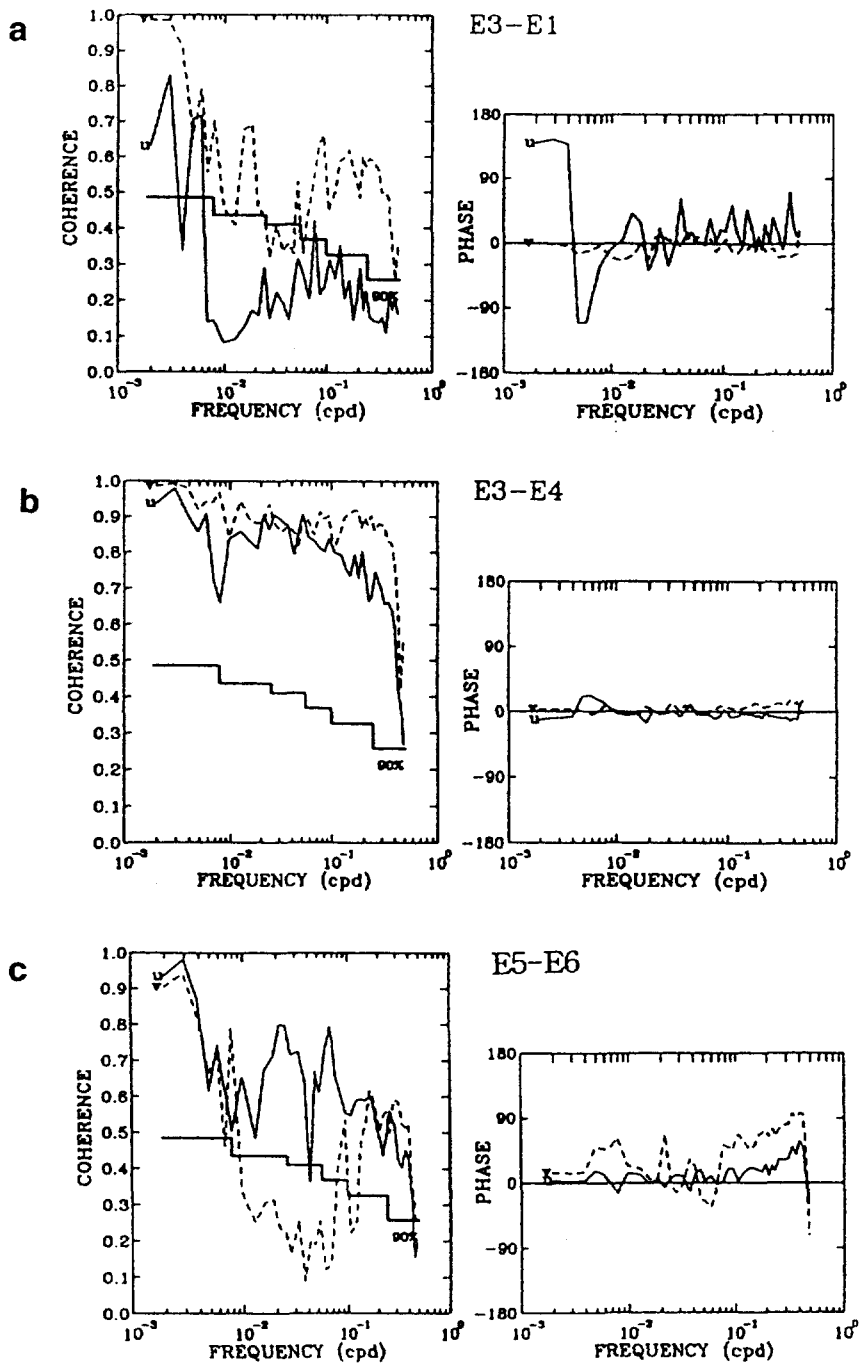

Fig. 8. Coherence and phase difference for wind stress for pairs of grids in the East Sea. (a) E3-E4. and (c) E5-E6. Solid and dashed lines correspond to the castward and northward components, respectively. The grids are marked in Fig.1

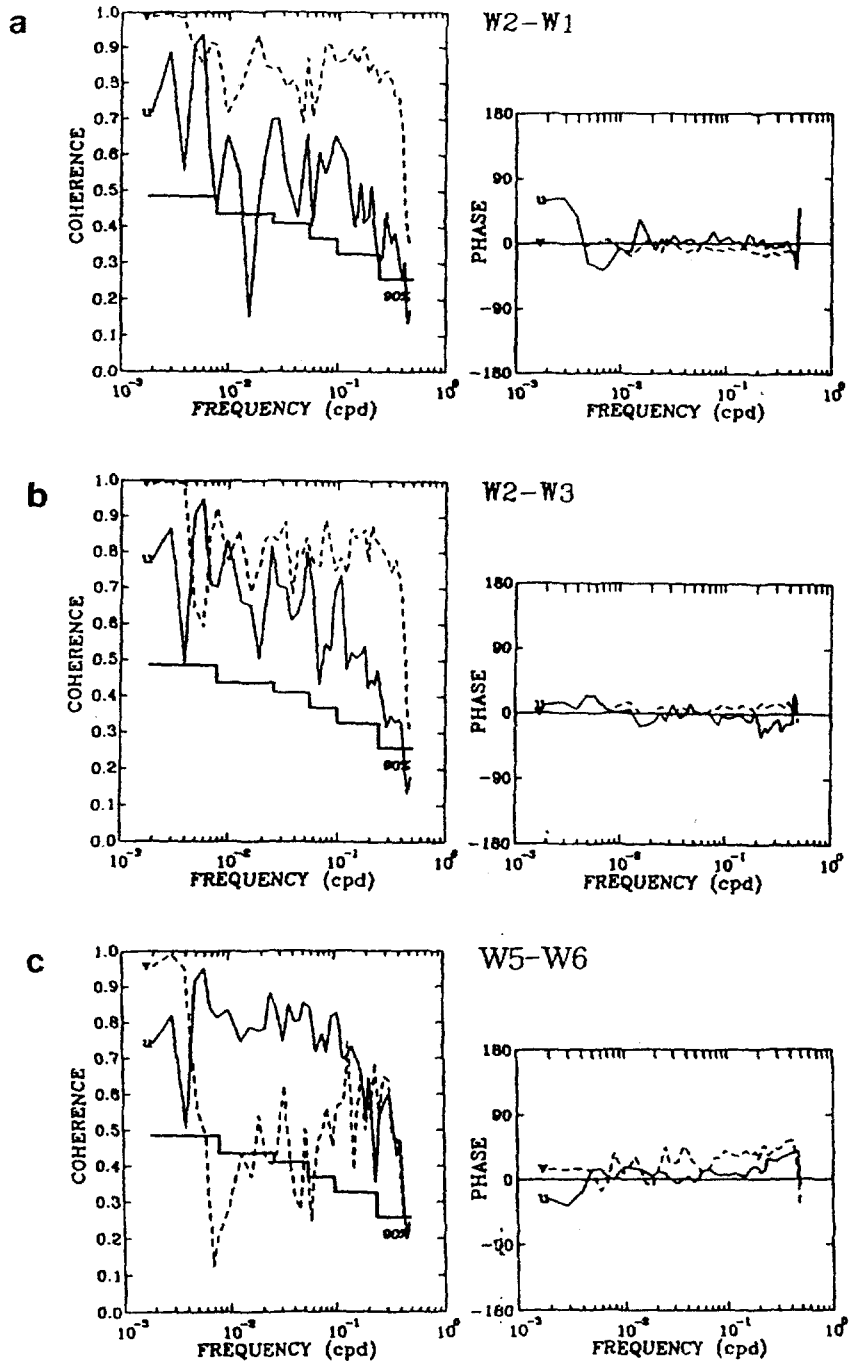

Fig. 9. Coherence and phase difference of winds for pairs of grids in the Yellow Sea. (a) W2-W1, (b) W2-W3, and (c) W5-W6. Solid and dashed lines correspond to the eastward and northward components, respectively. The grids are marked in Fig. 1.

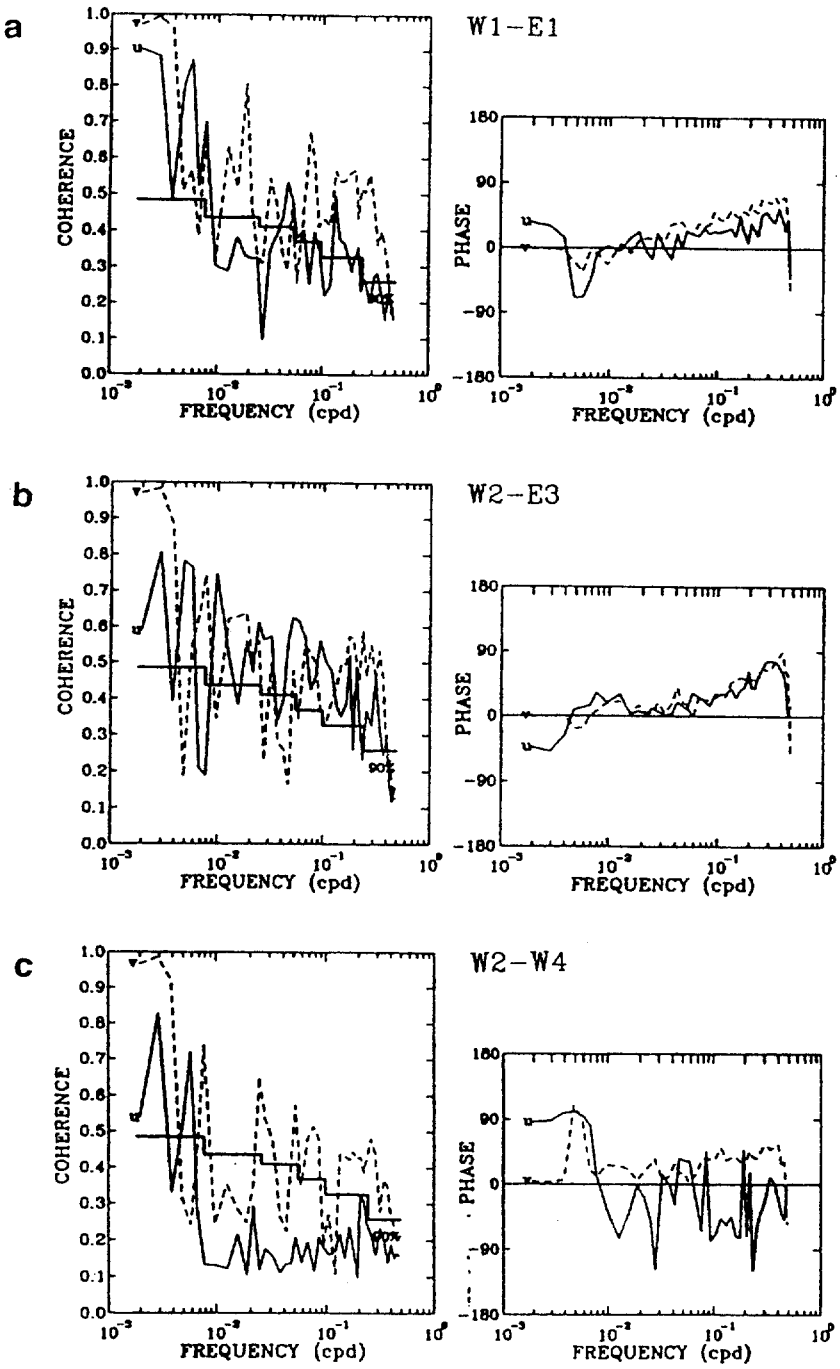

Fig. 10. Coherence and phase difference of wind stress between the Yellow Sea and East Sea or East China Sea (a) W1-E1, (b) W2-E3, and W2-W4. Solid and dashed lines correspond to the eastward and northward components, respectively. The grids are marked in Fig. 1.

cpy. For winds over YS and ECS which are not disturbed by the Korean peninsula, the north wind at 1 cpy is highly coherent with a very slight phase difference, even over a large distance between two grids W2 - W4. The east wind at 1 and 2 cpy is also spatially correlated with phase difference of about 90 degrees. The east wind at W4 advances that at W2 at both frequencies, which is different from the case for YS and ES. One remarkable feature is that for pairs of W1 - E1 and W2 - E3, phase increases linearly with frequency in the high frequency range larger than 0.02 cpd. Furthermore, the phases of both wind components are nearly the same over the frequency range. The systematic linear increase in phase is observed only for the two pairs of grids separated by the Korean peninsula.

CONCLUSIONS

The temporal and spatial characteristics of the sea surface wind fields over ES, YS, and ECS were investigated from gridded time series of daily wind data for a ten years period of 1978~1987. Spatial patterns of the long-term annual mean wind stress and curl have a strong resemblance with the long-term monthly mean structures during the winter season. The most pronounced periodicity is the annual cycle which explains for most of temporal variability. The synoptic wind field, dominated by the annual cycle is spatially very coherent over the neighbouring seas, but its basin-scale pattern differs to some extent from one basin to another one. During the winter season, the prevailing winds are northerly over the northern ES, northwesterly over the southern ES, northerly over the YS and the northern ECS, and northesterly over the southern ECS. At the same time, the wind stress curl is positive over the northern ES and southern ECS east of Taiwan, while it is negative over the southern ES, YS, and the northern ECS. During the summer season, the synoptic pattern changes completely, with the wind stress and curl being much reduced in magnitude. High variability in summer over the ECS results mainly due from frequent northward passage of tropical storms.

The semi-annual periodicity is characteristic of the synoptic winds over the study area. Its contribution to the total variance in time is much smaller than the primary periodicity at 1 cpy, but east winds are found to be locally affected by the secondary periodicity at 2 cpy, especially in YS and the southern ES where its spectral density is comparable to that of the annual periodicity. The semi-annual periodicity may reflect transit phases in spring and autumn of the phases at 2 cpy over each basin of ES, YS, and ECS propagates northward and the phase over YS advances that over ES, so the east wind is excepted to propagate from southwest toward northeast, in the opposit direction of the north wind at 1 cpy. Therefore, the semi-annual periodicity and its propagation direction are apparently coincident with those of the extratropical cyclones crossing the Korean peninsula which develop during the transit period. However, the predominant clockwise rotational motion at 2 cpy (Lie *et al.*, 1995) should be clarified.

There are no significant spectral peaks in the high frequencies. However, the cross-spectral analysis for pairs of grids in YS and ES with distance of about 900 km show that phases over YS lag behind those over ES in the frequencies higher than 0.1 cpd, its magnitude increasing linearly with frequency. The phase speed is estimated about 550 and 730 km/d at 0.1 and 0.3 cpd, with a westward propagation. Also the winds in higher frequencies are characterized by counterclockwise rotation motion (Lie *et al.*, 1995). The observed time scale, phase speed, and rotational motion have a good match with the characteristics of moving extratropical cyclones which frequently cross the Korean peninsula in the west-east direction. In the winter time, the cyclones were reported to develop more significantly in ES than in YS and ECS (Jung and Jhun, 1977), but more sophisticated analysis should be made to elucidate whether the phase and moving directions are coincident.

ACKNOWLEDGEMENTS

Authors would like to send their deep thanks to

Professor Tae-Young Lee, Yonsei University for his helpful and constructive comments on the manuscript. This study was supported partly by grants given to the second author (H. -J., Lie) from the Ministries of Science and Technology during 1993-1995 and from the Basic Research Program of Korea Ocean Research and Development Institute during 1993-1994. The third author (J. -Y., Na) also acknowledge partial support of the Ocean Research Institute Program, Ministry of Education in Korea, 1995 and from the Oceanographic Research Fund, Ministry of Education in Korea, 1995.

REFERENCES

Bunker, A. F., 1976. Computations of surface energy flux and annual air-sea interaction cycles of the North Atlantic Ocean. *Mon. Wea. Rev.*, **104**: 1122-1139.

Cardone, V. J., 1969. Specification of the wind distribution in the marine boundary layer for wave forecasting. New York Univ. School of Engineering and Science Rep. GSL-TR-69-1, 181pp.

Chave, A. D., D. S. Luther and J. H. Filloux, 1991. Variability of the wind stress curl over the North Pacific : Implications for the oceanic response. *J. of Geophys. Res.*, **96**(C10): 18,361-18,379.

Hidaka, K., 1958. Computation of the wind stress over the oceans. *Rec. Oceangr. Wks. Japan*, **4**: 77-123.

Hellerman, S., 1968. An updated estimate of the wind stress on the world ocean. *Mon. Wea. Rev.*, **95**: 607-614.

Jung, C. H. and J. G. Jhun, 1977. A study on the development of extratropical cyclones in the area of Korean peninsula. *J. Korean Meteoro. Soc.*, **13**: 1-12.

Kim, C. H. and B. H. Choi, 1986. Monthly wind stress and wind stress curl distributions in the Eastern Sea (Japan Sea). *J. Korean Association for Hydro. Sci.*, **19**: 239-248.

Kim, C. -H. and J. G. Jhun, 1992. Numerical simulations of the three-dimensional land and sea breeze under synoptic flows over South Korea, *J. Korean Meteoro. Soc.*, **28**: 165-181.

Kutsuwada, K., 1982. New computation of the wind stress over the North Pacific Ocean. *J. of Oceanol. Soc. Japan*, **38**: 159-171.

Lie, H. -J., J. Y. Na, S. K. Han and J. W. Seo, 1994. Monthly mean sea surface winds over the East China Sea. KORDI Rep. BSPE 00367-683-1, 91pp, (in Korean).

Lie, H. -J., J. Y. Na, and S. K. Han, 1995. Variabilities in time and space of sea surface winds around Korea. KORDI Rep. BSPE 00444-788-1, 53pp, (in Korean).

Na, J. Y., J. W. Seo and S. K. Han, 1992. Monthly-mean sea surface winds over the adjacent seas of the Korea Peninsula. *J. of the Oceanol. Soc. Korea*, **27**: 1-10.

Park, Y. -S. and S. -U. Park, 1991. Observational features of local weather in the coastal regions over South Korea in spring. *J. Korean Meteoro. Soc.*, **27**: 67-86.

Willebrand, J., 1978. Temporal and spatial scales of the wind field over the North Pacific and North Atlantic. *J. of Phys. Oceanogr.*, **8**: 1080-1094.

Wyrtki, K. and G. Meyers, 1975. The trade wind field over the Pacific Ocean. Part I. The mean field and the mean annual variation. Hawaii Inst. Geophys. Rep., HIG-75-1, Univ. Hawaii, 26pp.

Wyrtki, K. and G. Meyers, 1976. The trade wind field over the Pacific Ocean. *J. Appl. Meteor.*, **15**: 698-704.

Accepted January 10, 1996